Applied Physics Letters PERSPECTIVE pubs.aip.org/aip/apl

Copolymers for electronic, optical, and sensing applications with engineered physical properties

Cite as: Appl. Phys. Lett. **123**, 050501 (2023); doi: 10.1063/5.0141885
Submitted: 9 January 2023 · Accepted: 16 July 2023 ·
Published Online: 31 July 2023

View Online Export Citation CrossMark

Yuxuan Zhang and Sunghwan Lee[a)]

AFFILIATIONS

School of Engineering Technology, Purdue University, West Lafayette, Indiana 47907, USA

[a)]Author to whom correspondence should be addressed: sunghlee@purdue.edu

ABSTRACT

Electronic and optoelectronic devices often require multifunctional properties combined with conductivity that are not achieved from a single species of molecules. The capability to tune chain length, shape, and physicochemical characteristics of conductive copolymers provides substantial benefits for a wide range of scientific areas that require unique and engineered optical, electrical, or optoelectronic properties. Although efforts have been made to develop synthetic routes to realize such promising copolymers, an understanding of the process–structure–property relationship of the synthesis methods needs to be further enhanced. In addition, since traditional methods are often limited to achieving pinhole-free, large-area coverage, and conformal coating of copolymer films with thickness controllability, unconventional synthetic strategies to address these issues need to be established. This Perspective article intends to enhance knowledge on the process–structure–property relationship of functional copolymers by providing the definition of copolymers, polymerization mechanisms, and a comparison of traditional and emerging synthetic methods with reaction parameters and tuned physical properties. In parallel, practical applications featuring the desired copolymers in electronic, optical, and sensing devices are showcased. Last, a pathway toward further advancement of unique copolymers for next-generation device applications is discussed.

I. INTRODUCTION

Organic electronic and optoelectronic devices, such as organic field effect transistors, sensors, and solar cells, have progressed fast and have been practically integrated into organic logic devices, organic-light-emitting-diode displays, photodetectors, toxic compound detectors, and building-integrated organic photovoltaics. These applications often demand not only improved performance but also the integration of electrical conductivity with other properties desired from the active component of the device, which is commonly accomplished through the use of conductive copolymers.[1–4] The physical properties of copolymers are highly tunable during the synthesis process since the properties of copolymers are intermediate between those of the corresponding homopolymers, which is one of the main benefits of copolymers.[5,6] For achieving the demanded optical and electrical properties, several synthesis methods of copolymers have been well developed. Traditional solution-based chemical syntheses, electrochemical polymerization, and photoinitiated process have been widely reported and adopted in the polymerization process.[7,8] For the recently emerged method based on chemical vapor deposition, oxidative chemical vapor deposition has received particular attention for applications in optoelectronic and electronic devices due to the high conductivity and higher retention of organic functional moieties of the resulting copolymer.[9–13] In order to compare the capabilities of copolymer synthetic methods and suggest a universal selection rule, four widely considered processing methods are listed in Table I, with the characteristics often required for the resulting copolymers.

These synthetic methods mainly follow two polymerization mechanisms of chain-growth polymerization and step-growth polymerization.[16,17] In chain-growth polymerization, the monomers add onto the active site of a growing polymer chain, one at a time due to the limited active sites, which is the pivotal characteristic of this mechanism.[18,19] Generally, the chain-growth polymerization reaction must include the chain initiation and chain propagation process, which are illustrated in Fig. 1(a). The chain initiation is the generation of a chain carrier presented as a red circle, which can be a radical or an ion working as an intermediate.[20,21] Then, the reaction is carried on by the chain propagation process, during which one monomer (the blue circle) is added to form a polymer molecule with one repeat unit longer.[21] In contrast, step-growth polymerization [Fig. 1(b)] proceeds without an initiation process. Chain propagation reactions directly occur without an initiator. Reaction proceeds between pairs of monomers; a monomer and a dimer; a monomer and a longer chain; or between two n-mer chains.[22–24]

TABLE I. Comparison of synthetic methods of copolymers.

	Traditional solution-based chemical synthesis	Electrochemical polymerization	Photoinitiated process	oCVD
Residual-solvent-induced defects	Yes	Yes	Yes	No
Substrate independent	No	No	No	Yes
Interfacial grafting	Hard	Hard	Hard	Easy
Ultrathin (<10 nm) pinhole-free film	Hard	Hard	Hard	Easy
Thick film (>500 nm)	Easy	Easy	Easy	Hard
Copolymer nanoparticles[14,15]	Yes	Yes	No	No
System price	Low	Mid	Mid	High
Industrial capability	High	High	Mid	Low
Conformal coverage	Poor	Poor	Poor	Good
Reaction mechanism	Chain-growth polymerization step-growth polymerization	Step-growth polymerization	Chain-growth polymerization	Step-growth polymerization
Resulting copolymer type	Conjugated- and non-conjugated polymers	Conjugated polymers	Non-conjugated polymers	Conjugated polymers

The consumption of monomers in step-growth polymerization is fast, and the degree of polymerization (i.e., the chain length) is gradually increasing during the whole polymerization process.[25,26] The monomer adopted in step-growth polymerization reaction should have functional groups that enable the step by step adding of the monomer to the growing polymer.[27] Attributed by the different aggregation process, monomers in chain-growth polymerization can only be added on the site of "reactive center" of a molecule (e.g., monomer and growing chain).

The synthesized copolymer backbones can be linear or display more complex chain architectures, which lead to different optical and electrical properties.[28–31] The monomers may link in blocks, alternate, or form statistical sequences, as schematically illustrated in Fig. 2 ①–③, respectively.[32–34] Copolymers with branched chain architectures including graft copolymers (Fig. 2 ④) and star copolymers (Fig. 2 ⑤) are also presented.[35,36]

The chain architectures are largely dependent on the reaction parameters, such as monomer selection, the ratios of incorporated monomers, and the sequence of incorporation and reaction conditions (e.g., temperature, pH value, and reaction time) within the synthesis process. However, the process–structure–property relationship has not been fully established yet, which is essential to strategically design and manipulate the desired properties of copolymers for further advancement in electronic and optoelectronic applications. In addition, traditional synthetic methods are often limited to realize pinhole-free, large-area coverage, and conformal copolymer films with thickness controllability on various substrates.

Herein, we compare the characteristics and reaction factors of those major synthesis methods for copolymers to systematically understand their mechanism and, hence, strategically design the polymerization process. First, the synthetic route and milestones of each method are elaborated and presented in the company of the practical applications of the copolymers with desired optical and electrical properties. More importantly, the process parameters (e.g., reactants, voltage range, and lighting conditions) for achieving preferable optical and electrical properties are discussed to provide guidance for tuning these physical properties of copolymers. As an emerging synthetic method, oxidative chemical vapor deposition is also discussed to achieve pinhole-free copolymer films on various substrates with controllable thickness for high performance electronic and optoelectronic devices. Finally, we propose the development pathways of synthetic methods and potential applications of copolymers.

II. CONVENTIONAL CHEMICAL SYNTHESIS

Among the traditional polymerizations, chemical synthesis is the most adopted method and has been well evolved. A general synthetic process requires a series of chemical reactions to convert monomers into copolymers by generating covalent bonding, where the optical and electrical properties of the synthesized copolymer can be modified through the tuning of the reactant ratio and reaction conditions.[37–39] It has been demonstrated through chemical synthesis that the optical and electrical properties of a copolymer were engineered by porosity of the resulting copolymer. By optimizing the pH value of the reaction solution and the molecule weight of monomers, Cho *et al.* controlled the porosity of the synthesized copolymer to achieve high light transmission for potential applications in antireflective films, sensors, and optoelectronic devices.[40] To build block copolymers for selectively and reversibly controlling the transmission of light, they adopted polystyrene-block-poly(4-vinylpyridine) (denoted PS-b-P4VP) and anionic polystyrene-block-poly(acrylic acid) (denoted PS-b-PAA) as two segments of the copolymer films. The copolymer films of poly[(PS-b-P4VP)-co-(PS-b-PAA)], which are prepared at pH 4 for PS-b-P4VP and at pH 6 for PS-b-PAA, have the highest porosity compared with those synthesized at different pH conditions. Figure 3(a) illustrates the achieved highly nanoporous structure of the poly[(PS-b-P4VP)-co-(PS-b-PAA)] copolymer films. According to the height and phase images of atomic force microscopy (AFM) in Fig. 3(a), the highly nanoporous copolymer film is formed by ten bilayer-merged micelles, of which the porosity led to the light transmission of more than 99%.

Inducing sacrificial template in conventional chemical synthesis also demonstrates the capability to change the optical and electrical properties of the copolymer thin film. By introducing inorganic Fe_3O_4

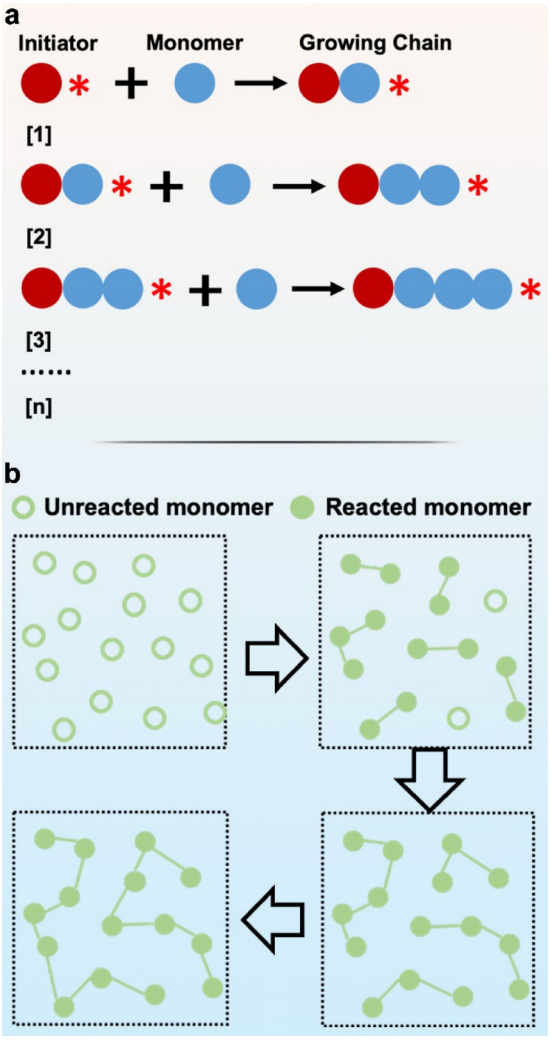

FIG. 1. (a) Schematic of the mechanism of chain-growth polymerization. (b) Schematic of the mechanism of step-growth polymerization (the hollow circle and solid circle represent the unreacted and reacted monomers, respectively).

nanoparticles during the copolymerization process, Kim and Yoo create composite architecture for the copolymer as indicated in Fig. 3(b), which were subsequently removed with a post-acid treatment.[41] The introducing and dissolving Fe_3O_4 particles generated functional pores, which work as nano-conducting channels in the block copolymer of poly[(ether-ether-ketone)-co-(hexafluoroisopropylidene)diphenol-co-decafluorobiphenyl]. The proton conductivity and ion exchange capacity were remarkably enhanced by the generated porous structure.

However, the solution-based chemical polymerization process may be limited due to the inevitable process of evaporating the residual liquid since dewetting defects, such as the pinhole, on the synthesized polymer are often generated. The surface tension of liquid often causes the ununiform thickness of the synthesized polymer.[42] In addition, thin film conjugated copolymers that are typically required for many of the electronic and optoelectronic devices cannot be synthesized by

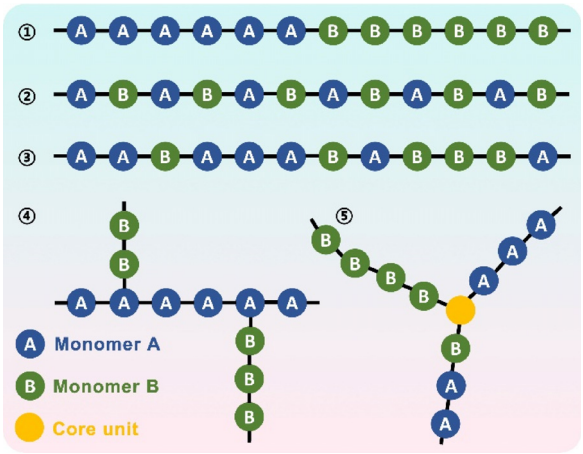

FIG. 2. Schematics of various copolymers (①: block copolymer, ②: alternating copolymer, ③: random copolymer, ④: branch copolymer, and ⑤: star copolymer).

conventional chemical synthesis methods, resulting in copolymers generally in the form of insoluble powders.

III. ELECTROCHEMICAL SYNTHESIS

The synthetic electrochemistry of copolymers has received a lot of attention since the 1980s due to the electrolysis phenomenon that is the chemical reaction driven by the applied direct electric current, leading to the changes in the structure of electroactive macromolecules. Electrochemical synthesis provides an efficient way to realize selective oxidative or reductive transformation with electrons working as reactants, which is beneficial in that it excludes harsh and often toxic reagents, compared to solution-based chemical syntheses.[43,44] A typical electrochemical synthesis apparatus is constituted of a reactor where the reaction solution (solvent and electrolyte) and two electrodes connected with a power supply are typically inlcuded.[45–47] Within the polymerization process, the coupled electrochemical reactions occur separately on the working electrode and counter electrode as demonstrated in Fig. 3(c). Electrochemical synthesis manipulates the activity of the reagent through the potential of the electrode. There are two different ways to control electrochemical synthesis, i.e., potentiostatic and galvanostatic processes. Specifically, during the potentiostatic process, the electrode potential is set on the plateau of the transition from reactants to products (i.e., monomers to polymers in polymerization), and then the current and the reactant concentration will decrease as polymerization proceeds and then eventually reaches zero.[48,49] Under the galvanostatic condition, the oxidation current is set below the polymerization current to make the electrode potential suitable for the required reactions.[50] The optical and electrical properties of copolymers synthesized through electrochemical polymerization are governed by the process conditions such as monomer concentration ratios, solvent concentrations, and applied potentials. The resulting copolymer may exhibit the characteristics of all monomers (or their homopolymers) used in the copolymerization synthesis or synergistically enhanced performance.[51,52] For example, a copolymer of poly[pyrrole-co-(poly-N-(p-nitrophenyl)pyrrole)] electrochemically generated on the Pt electrodes from an acetonitrile solution is equipped with a similar electrochemical behavior of both

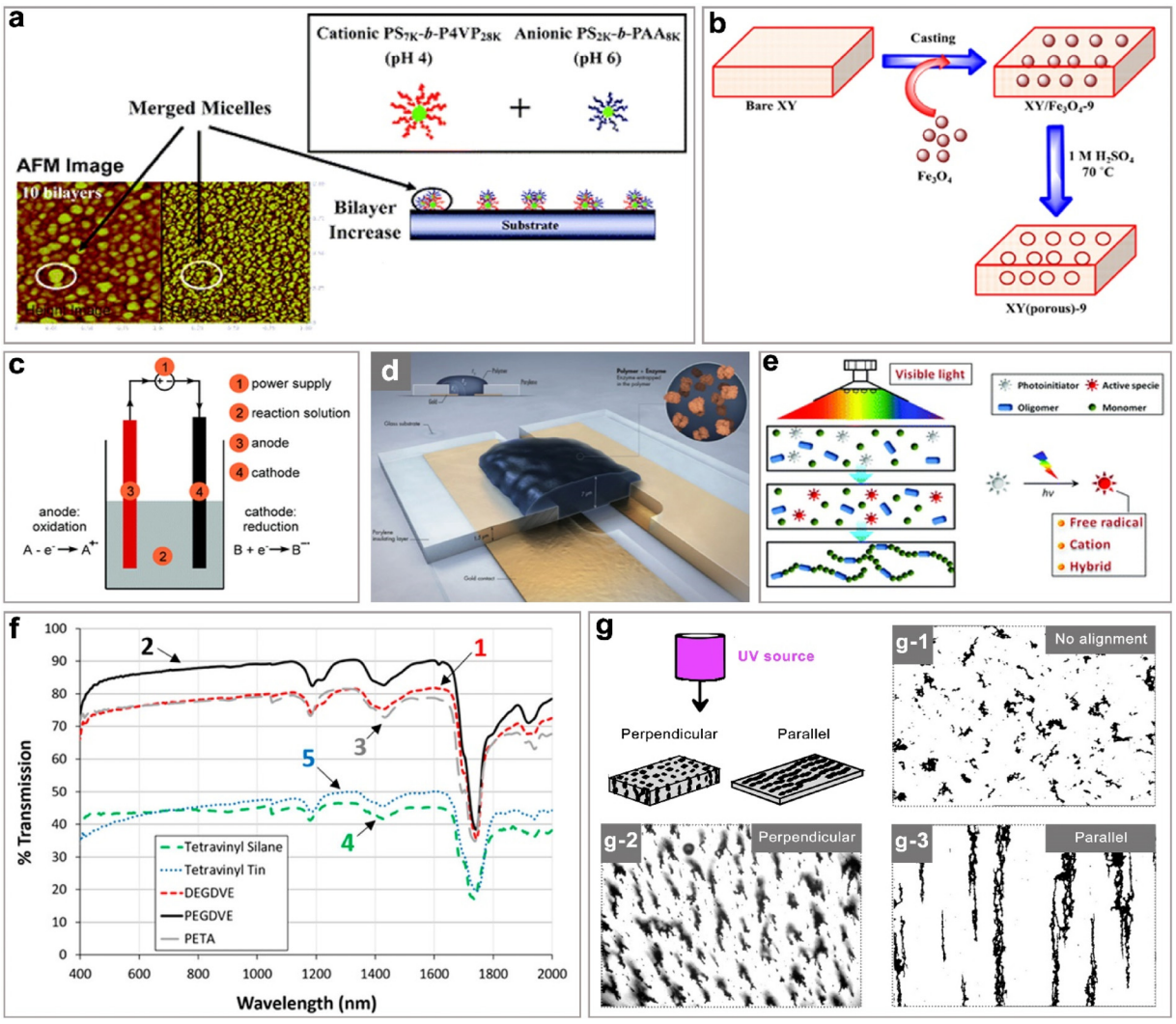

FIG. 3. (a) AFM images and schematic illustration of the self-assembly of nanoporous poly[(PS-b-P4VP)-co-(PS-b-PAA)] multilayer films formed at pH 4 and pH 6 via conventional chemical synthesis by increasing the number of bilayers.[40] Reproduced with permission from Cho *et al.*, J. Am. Chem. Soc. **128**, 9935 (2006). Copyright 2006 American Chemical Society. (b) Preparation process of XY(porous)-9 membrane through conventional chemical synthesis.[41] Reproduced with permission from Kim and Yoo, Polymers **11**, 563 (2019). Copyright 2019 MDPI. (c) Schematic of electrochemical synthesis representing red-anode; black-cathode; and grey-reaction solution.[47] Reproduced with permission from Schotten *et al.*, Green Chem. **22**, 3358 (2020). Copyright 2020 Royal Society of Chemistry. (d) Schematic of the conducting polymer composite grown in the organic electrochemical transistor channel synthesized by electropolymerization.[59] Reproduced with permission from Wustoni *et al.*, Adv. Mater. Technol. **5**, 1900943 (2022). Copyright 2020 Wiley-VCH. (e) Schematic of photoinitiated polymerization.[64] Reproduced with permission from Shao *et al.*, Polym. Chem. **5**, 4195 (2014). Copyright 2014 Royal Society of Chemistry. (f) UV–vis–NIR plots compared between various synthesized copolymers through photoinitiated polymerization.[66] Reproduced with permission from McClain *et al.*, Ind. Eng. Chem. Res. **57**, 8902 (2018). Copyright 2018 American Chemical Society. (g) Schematic of the distribution of perpendicular and parallel alignment of the nickel particles in the sample synthesized by photoinitiated polymerization.[67] Reproduced with permission from Knaapila *et al.*, ACS Appl. Mater. Interfaces **6**, 3469 (2014). Copyright 2014 American Chemical Society. (g-1)–(g-3) Optical micrographs of alignment of nickel particles in the sample, (g-1) no alignment, (g-2) perpendicular alignment, and (g-3) parallel alignment.[67] Reproduced with permission from Knaapila *et al.*, ACS Appl. Mater. Interfaces **6**, 3469 (2014). Copyright 2014 American Chemical Society.

nitrobenzene and polypyrrole.[53] For an electrochemically assembled copolymer of poly(thiophene-co-pyrrole), the conductivity of the synthesized copolymer is higher than the homopolymers of polythiophene and polypyrrole.[54]

Electrochemical polymerization has been considered to synthesize functional copolymers for, in particular, electrochemical applications, such as electrochromic devices, biosensors, and energy storage devices.[55–57] For instance, the poly[(terphenyl bridged-SNS)-co-(3, 4-ethylenedioxythiophene)] [poly(TPhSNS-co-EDOT)] exhibited higher electrochemical stability and higher electrochromic property than the TPhSNS homopolymer, which maintained color for longer than 36 h stably, potentially applicable in electrochromic devices.[58]

Electrochemical polymerization also demonstrated capability to directly fabricate electronic devices by adjusting the reactor configuration

and the reaction conditions. Wustoni *et al.* assembled *in situ* biofunctionalized conducting copolymer films as transistor channels by tuning the shape of the reaction container and the content of the reaction solution [Fig. 3(d)].[59] The solution containing a mixture of 3,4-ethylenedioxythiophene (EDOT), hydroxymethyl EDOT (EDOTOH), and catalytic enzymes was dropped in microscale channels, and it generated the copolymer p(EDOT-co-EDOTOH) via an electrochemical polymerization process. Consequently, the catalytic enzymes were entrapped in the copolymer to work as analyte immobilizing medium in metabolites sensors. The sensor exhibited a high sensitivity to the glucose content in the phosphate buffered saline solution, which ranged from 10×10^{-6} to 10×10^{-3} M, with consistent performance over 2 months.

Understanding the relationship between the potential of the electrode and the behavior of copolymerization is vital to the synthetic process and needs to be further enhanced to realize desired copolymers for the targeted applications. In a recent potentiostatic electrolysis study, the controlling of the ring-opening copolymerization was demonstrated through the engineering of the reactivity of monomers. In addition, the structure of the polymer backbone can be tuned through the successive applications of an electric potential during the copolymerization process, by which the molecular weight distribution of block copolymers may be controlled.[60] This precise controlling of connectivity monomers may serve as a method of copolymerization for facile electronic device implementation.

Despite the demonstrated benefits, limitations of electrochemical synthesis still exist for the implementation in a wide range of device applications. First, electrochemical synthesis is only available with electrically conductive substrates to process the copolymerization. Moreover, the electrolyte, which promotes the ion transfer in the solution during the electrochemical synthesis process, is often not available.[61]

IV. PHOTOINITIATED POLYMERIZATION

Photoinitiated polymerization has gained attention due to the combined economic and sustainable ecological expectations. Light is the initiator in the chain-growth process of photoinitiated polymerization by generating initiating radicals. For ending the chain growth, terminal radicals are required.[34] A photoinitiator is mandatory to be added into the monomer solution to originate the photoinitiated polymerization since most monomers are not able to generate the polymerization after light irradiation.[62,63] As indicated in Fig. 3(e), the photochemical reaction starts with the photo absorption of the photoinitiator molecule at the ground state (of which the energy is defined as $h\nu$, where h is the Planck constant and ν is the frequency of light), then an electron will be excited from the highest occupied molecular orbital (known as HOMO) of the photoinitiator molecule into a higher orbital and generate the first singlet-excited-state molecule (active species), which produce free radicals from primary photochemical processes.[64] These free radicals suffer thermal propagation reactions with monomers to yield polymers and continually propagate the polymerization until the absence of light. The optical and electrical properties of the synthesized copolymer largely depend on the types and relative ratio of monomers. With the same synthesis conditions, the resulting copolymers with different monomer ratios and varying monomer kinds exhibited altered electrical and optical properties.[65,66] McClain *et al.* employed diethylene glycol divinyl ether (DEGDVE), polyethylene glycol divinyl ether (PEGDVE), pentaerythritol tetraacrylate (PETA), tetravinylsilane (TVSi), and tetravinyltin (TVSn) to copolymerize with pentaerythritol tetrakis(3-mercaptopropionate) (PETMP), respectively.[66] The poly(PETMP-co-DEGDVE) (copolymer 1), poly(PETMP-co-PEGDVE) (copolymer 2), and poly(PETMP-co-PETA) (copolymer 3) have high transmission, greater than 75% in the visible and near-infrared regime, as evaluated by UV-vis-NIR analysis [Fig. 3(f)]. However, poly(PETMP-co-TVSi) (copolymer 4) and poly(PETMP-co-TVSn) (copolymer 5) were far less transmissive, which might be ascribed to the semimetal silicon in TVSi and the metal tin in TVSn. The high transmission achieved from copolymer 1, 2, and 3 enables their applications in optical coatings and soft imprint lithography.

Photoinitiated polymerization is difficult to process conjugated polymers. Introducing metal particles may provide the electrical conductivity in the photosynthesized copolymers. However, metal particles may lead to lower optical transmission, which results in the longer curing time. Moreover, the distribution of metal particles in copolymers, which is hard to control, will affect the optical and electrical properties of the resulting copolymer. Coupling with other physical fields synergistically can be effective in mitigating issues caused by foreign matters, thus adjusting optical and electrical properties of copolymers. The magnetic field has been verified to be capable for controlling the alignment of the nickel particles to form chainlike pathways through the sample as illustrated in Fig. 3(g).[67] As verified by optical microscope image in Fig. 3(g-1), the nickel particles distributed randomly in the sample synthesized without magnetic field. For samples prepared with magnetic fields, the alignment of nickel particles is enhanced due to the presence of the magnetic fields, showing perpendicular and parallel particle chains as indicated by Figs. 3(g-2) and 3(g-3), respectively. The conductivity of samples largely depends on the alignment direction of nickel particles, specifically samples with paralleled nickel alignment have much higher conductivity compared with those with perpendicular alignment. Lower nickel particle fraction may improve the transparency and lessen the curing time with maintaining of conductivity.

The restricted choice of the capable monomers is the main weakness of photoinitiated polymerization, restricting the functionality of the synthesized polymer. Particularly, it is crucial for the monomer to be compatible with the photoinitiators in order to prevent any potential side reactions. Furthermore, it is important that the monomer demonstrates adequate photostability, exhibiting no spontaneous polymerization or degradation reactions under light. This ensures that the polymerization reaction takes place exclusively under controlled conditions. The approach of incorporating metal particles is rather indirect mitigation, and the assistance of magnetic field is not trivial and expensive, which is not favored for copolymerization. The photoinitiated synthesis process is further limited to engineer the properties of the resulting copolymers, such as dimensions and biocompatibility, due to the toxicity of the resins required for the photoinitiated polymerization.[11,64,68]

V. OXIDATIVE CHEMICAL VAPOR DEPOSITION

Oxidative chemical vapor deposition (oCVD) offers a single step process of polymer synthesis, deposition, and doping of many promising conjugated polymers. A step-growth polymerization through oCVD is enabled by the reaction between the oxidizing agent and monomers, from which the cation radicals of the monomer unit are

generated.[69,70] Then, pairs of cation radicals dimerize and deprotonate via reactions with oxidants to form neutral conjugated species.[71] The higher-order oligomers are then yielded through a series of continuous stepwise reactions of monomers and other oligomers and form conducting polymers with ever longer chains. As illustrated in Fig. 4(a), the synthetic route of poly(EDOT) (PEDOT) through the oCVD technique is a representative step-growth polymerization process as described above.[72]

A typical oCVD setup is generally constituted by a vacuum chamber with one or several monomer inlet ports as well as vacuum pumps on the side and at least one oxidant source at the bottom as illustrated in Fig. 4(b).[73] Before the deposition, the monomer will be loaded into the monomer jar [denoted as 1 in Fig. 4(b)], and the oxidant will be filled into another monomer jar or the oxidant crucible [denoted as 2 in Fig. 4(b)] depending on the state of the oxidants. Then, the source monomers and oxidants (either liquid or solid phase) will be vaporized. The substrate will be placed on a rotatory temperature-controlled stage. During the deposition, the temperature of the stage will be set typically from 25 °C (or room temperature) to 150 °C, by which the polymer conjugation may be engineered, and the pressure inside the chamber is preserved usually within the regime of 1–100 mTorr.[42,74,75] During the oCVD process, the electrical, chemical, and optical properties of the synthesized polymers are systematically tuned by reaction parameters, such as the flow rates of the vapor phase matters in the heated, the substrate temperature, and the overall chamber pressure.[76,77] The oCVD technique has showcased incomparable benefits in polymer coating [Fig. 4(c)], such as superior conformality on nonplanar structures, free from solvent-related defects, precise thickness controllability, and enhanced and tunable polymer properties.[42] The readily achieved conformal coverage of oCVD polymers affords complete protection and functionalization for nonplanar geometries for various electronic and optoelectronic applications including 3D printed electronics, medical sensors, and energy storage devices. Zhang *et al.* demonstrated the conformality and multifunctionality of oCVD PEDOT for the cathode in the lithium-ion battery.[78] The PEDOT layer was identified uniformly and conformally coated on both the microscale (cathode active materials, i.e., secondary particle) and nanoscale (gaps and voids between primary particles)

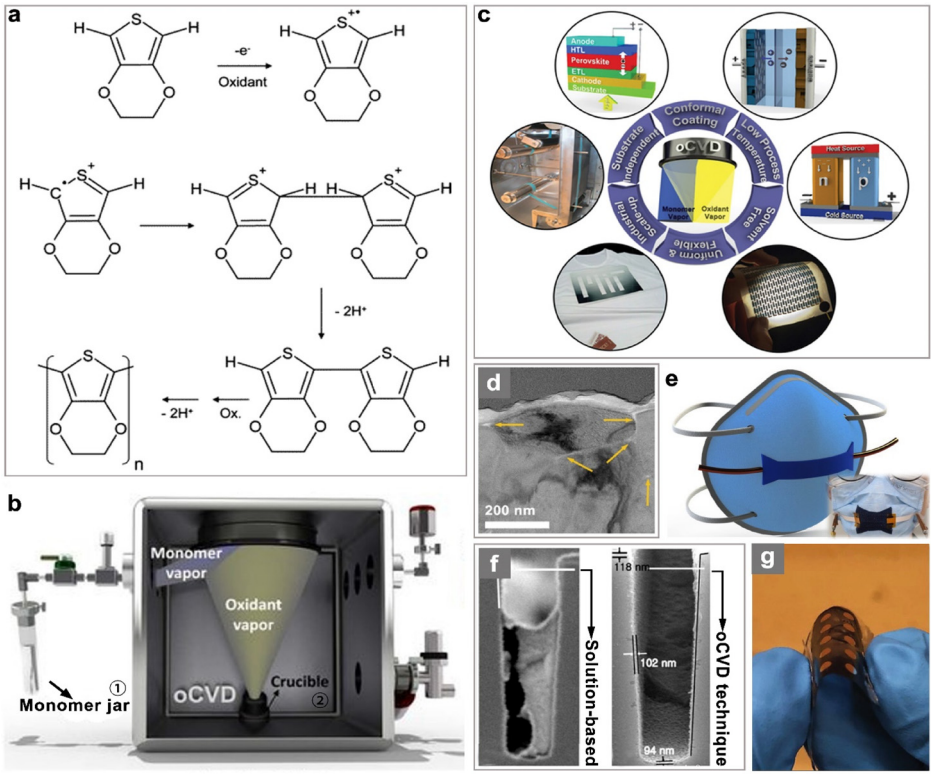

FIG. 4. (a) The step-growth mechanism of the oxidative polymerization of PEDOT.[72] Reproduced with permission from Im and Gleason, Macromolecules **40**, 6552 (2007). Copyright 2007 American Chemical Society. (b) Schematic illustration of oCVD reactor.[73] Reproduced with permission from Gharahcheshmeh *et al.*, Sci. Adv. **5**, eaay0414 (2019). Copyright 2019 AAAS. (c) Schematic of unique characteristics of oCVD (inner ring) and related applications of oCVD polymers.[42] Reproduced with permission from Gharahcheshmeh and Gleason, Adv. Mater. Interfaces **6**, 1801564 (2019). Copyright 2019 Wiley-VCH. (d) TEM image of oCVD polymer conformally coated on cathode active materials (white matter with yellow arrows between the cathode primary particles).[78] Reproduced with permission from Zhang *et al.*, Energy Storage Mater. **48**, 1 (2022). Copyright 2022 Elsevier. (e) Schematic and photo images of the oCVD polymer sensor fabricated on a disposable mask.[79] Reproduced with permission from Clevenger *et al.*, Sci. Adv. **7**, eabj8958 (2021). Copyright 2021 AAAS. (f) PEDOT films coated by solution-based synthesis (left, non-conformal) and oCVD technique (right, highly conformal) on a silicon trench wafer.[81] Reproduced with permission from Im *et al.*, ACS Nano **2**, 1959 (2008). Copyright 2008 American Chemical Society. (g) Photograph of the flexible photovoltaic device, leveraging oCVD PEDOT.[82] Reproduced with permission from Tavakoli *et al.*, Adv. Mater. Interfaces **7**, 2000498 (2020). Copyright 2020 Wiley-VCH.

enhancing the electrochemical stability of the battery as indicated in Fig. 4(d). In addition, the oCVD PEDOT offers the function of an electronic conductor in the cathode. Additionally, oCVD polymers can be directly deposited on various substrates including fabric and plastic since the low synthesis temperature may not lead to the thermal degradation of the substrate material. The deposited substrate is eligible to be directly applied as a part of the electronic devices. Clevenger *et al.* assembled wearable sensors on everyday fabrics by adopting the oCVD technique.[79] They deposited the PEDOT layer on various fabrics, of which the mechanical stability and breathability were conserved. These well-preserved features enabled the realization of the fabricating of blood pressure- and respiratory rate-monitoring sensors by using deposited gloves and masks [Fig. 4(e)]. The versatile processing avoids the possible residual solvent in the synthesized polymers and eliminates the pinhole defects led by dewetting phenomena, particularly for the fabrication of ultrathin polymer film. On the contrary to the solvent surface tension in solution-based synthesis, often leading to poor step coverage (i.e., inferior conformality) as shown in Fig. 4(f) (left), the polymer through oCVD is conformally deposited along the top, bottom, and sidewalls of the trench wafer, with a uniform thickness about 100 nm [Fig. 3(f), right].[80,81] In addition, the oCVD-deposited polymer is readily to be integrated into the device directly, as demonstrated in Fig. 4(g), where the polymer was deposited on the graphene and then assembled into photovoltaic device without any posttreatment while maintaining excellent flexibility desired in potential flexible and wearable electronics.[82]

The oCVD technique allows for a wide range of functional copolymerization by simply introducing additional monomer(s) that features desired properties. The electrical and optical properties of the resulting copolymers are governed by the types of monomers and functional groups involved in the copolymerization as well as the relative ratios of induced monomers.[8] Vaddiraju *et al.* reported the realization of a –COOH functionalized conducting copolymer through the oCVD technique in which monomers of pyrrole as well as thiophene-3-acetic acid (TAA) were co-vaporized in separate monomer jars with $FeCl_3$ as the oxidant, resulting in copolymerized films of poly(pyrrole-co-TAA).[83] Flow rates of the pyrrole and TAA monomers into the chamber were regulated to manipulate the concentration of TAA and the amount of –COOH in the copolymer. The copolymer films showed higher conductivity ($0.306\,S\,cm^{-1}$) compared with $10^{-4}\,S\,cm^{-1}$ of the homopolymer TAA. The enhanced conductivity is due to the larger quantity of pyrrole than that of TAA in the copolymer films since the polypyrrole is the more conducting component of the copolymer. Compared with polypyrrole homopolymer, the synthesized copolymer retained the functional groups –COOH, which can accommodate higher loading of silver nanoparticles. The realized oCVD-based conducting copolymer platform with high conductivity and robust attachment benefited the fabrication of resistance-based sensing devices due to the analyte immobilization capability of attached metal particles. Sensors employing similar approaches are provided below.

Afterward, they substituted the pyrrole monomer with EDOT monomers and manufactured the poly(EDOT-co-TAA) copolymer films.[84] The -COOH functional group was induced to grab the nickel (Ni) or palladium (Pd) nanoparticles through the formation of amide bonds between the –COOH groups and the amide groups of the functionalized metal nanoparticles as described in Fig. 5(a). Then, the selective response to volatile organic compounds (VOCs) of toluene and acetone was achieved by Ni/poly(EDOT-co-TAA)- and Pd/poly(EDOT-co-TAA)-based VOC sensing devices, respectively. This synthesis strategy provides a succinct way to assembling VOC devices with high sensitivity, excluding complicated polymer chemistries or device configurations.

To increase the sensitivity of oCVD copolymer-based sensors for a wider range of applications, such as the detection of biomolecules, Bhattacharyya and Gleason replaced metal nanoparticles in the metal-polymer hybrid system with bovine serum albumin (BSA) and showcased an all polymer-based sensing platform.[85] The covalent bonding was generated between BSA and the –COOH group on the poly(EDOT-co-TAA) copolymer, which was confirmed by high-resolution x-ray photoelectron spectroscopy (XPS) analysis for the N 1s orbital, shown in Fig. 5(b). The presence of characteristic peaks at 399.7 and 400.4 eV were attributed to –NH and N–C=O in poly(EDOT-co-TAA), identifying the covalent bond between BSA and the conducting copolymer. No peaks are visible in the oCVD copolymer without BSA attachment. Furthermore, the bromine gas was used as an oxidant agent so that the post rinse step required for the removal of residual $FeCl_3$ was eliminated, and the conductivity of the copolymer was improved to $\sim 10\,S\,cm^{-1}$, of which the higher conductivity is more suited for flexible biosensors with enhanced sensitivity.

To improve the signal-to-noise ratio so that the sensitivity of the sensor and the conductivity of the copolymer was further enhanced, TAA was replaced with 3-thiopheneethanol (3TE) and the –OH function group was incorporated in the oCVD copolymerization process.[86] The conductivity of poly(EDOT-co-3TE) had been improved by the substitution of TAA with TE. The resistance-based sensing device employing the poly(EDOT-co-3TE) copolymer [Fig. 5(c)] demonstrated reduced response time with the combination of electro-spun fiber mat only at nano-molar concentration. The structure of copolymer poly(EDOT-co-3TE) is demonstrated in Fig. 5(d). Additionally, the –OH functional groups on the surface of the copolymer exhibited the capability of the formation of covalent binding with inorganic, organic, or biomolecules, which is promising for various applications. For example, the poly(EDOT-co-3TE) was assembled into a rapid-detection device for food-borne pathogens, which provides both conductivity and antibody attachment capability, required for sensing. In addition, the achieved copolymer was identified to be nontoxic to humans through cytotoxicity evaluations.[87]

The effect of the ratio of the two monomers in the poly(EDOT-co-3TE) was further investigated by Goktas *et al.* Density functional theory (DFT) calculation confirmed that the combination of 3TE and EDOT is more kinetically preferable than the combination of two 3TE molecules.[88] The copolymerization of EDOT and 3TE was only available on the 2, 5 positions of the thiophene ring [marked in Fig. 5(e)] of the EDOT monomer since the ethylenedioxy ring, located on the 3, 4 positions of the thiophene ring, stabilizes the backbone structure of EDOT and 3TE and, hence, makes copolymerization difficult. The conductivity of the copolymer was systematically increased by decreasing the 3TE/EDOT monomer ratio (i.e., with increasing EDOT concentration in the copolymer), and high conductivity of $122\,S\,cm^{-1}$ was achieved when the 3TE/EDOT monomer ratio was 1/3. It is also observed that the optical properties of the poly(EDOT-co-3TE) are also tuned by the amount ratio between used monomers.[88] As EDOT increased in the copolymer, the color of the copolymer was tuned

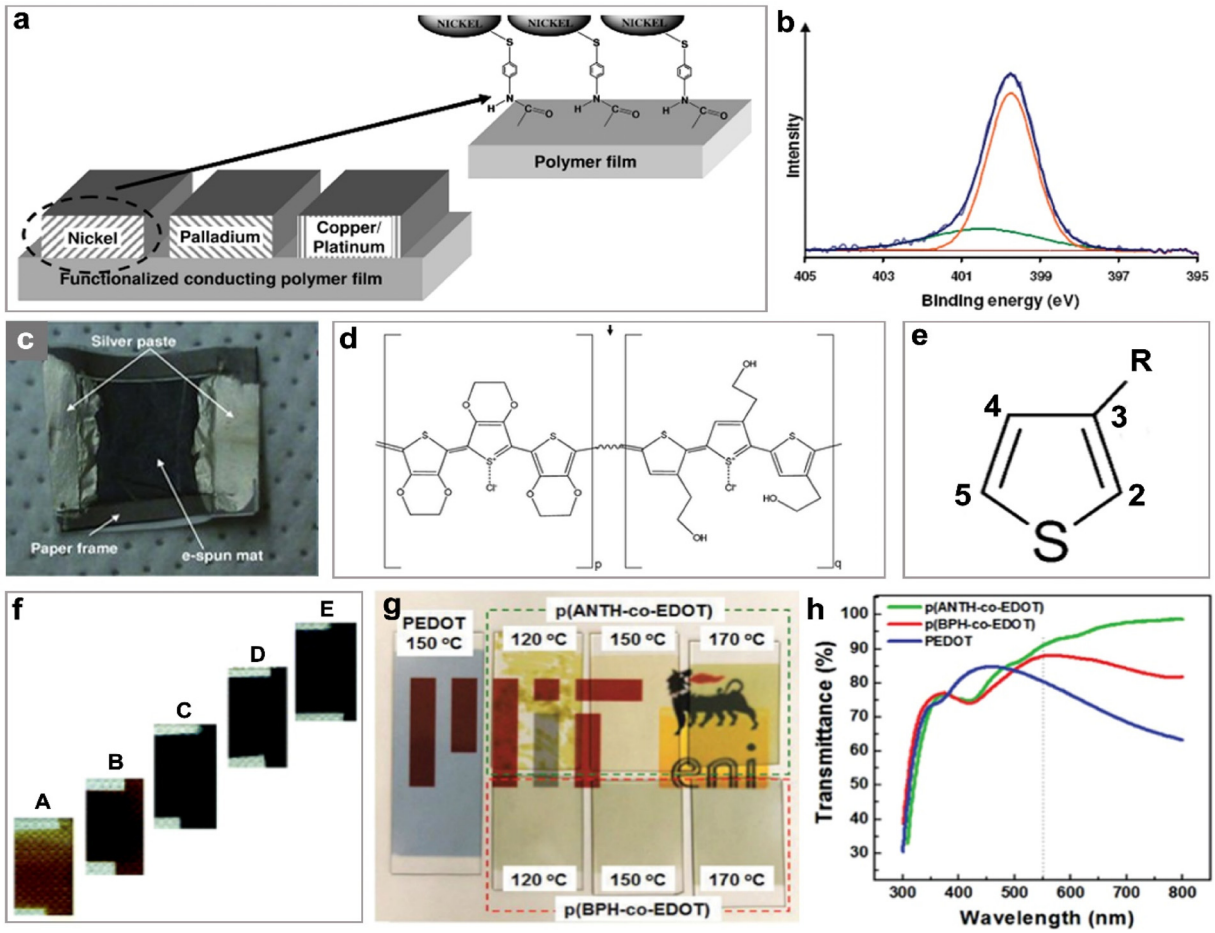

FIG. 5. (a) Pictorial illustration of a multigas/vapor sensor based on a oCVD conducting polymer-metal nanoparticle hybrid.[84] Reproduced with permission from Vaddiraju and Gleason, Nanotechnology **21**, 125503 (2010). Copyright 2010 IOP Publishing. (b) XPS C1s high-resolution spectra of BSA-attached poly(EDOT-co-TAA).[85] Reproduced with permission from Bhattacharyya and Gleason, Chem. Mater. **23**, 2600 (2011). Copyright 2011 American Chemical Society. (c) Schematic presentation of the fabrication steps of e-spun mat-based resistive biosensor.[86] Reproduced with permission from Bhattacharyya *et al.*, Adv. Funct. Mater. **21**, 4328 (2011). Copyright 2020 Wiley-VCH. (d) Structure of the copolymer poly(EDOT-co-3TE).[86] Reproduced with permission from Bhattacharyya *et al.*, Adv. Funct. Mater. **21**, 4328 (2011). Copyright 2020 Wiley-VCH. (e) The numbering convention of a thiophane ring with a substituent functional group on site 3.[88] Reproduced with permission from Goktas *et al.*, J. Mater. Chem. C **4**, 3403 (2016). Copyright 2016 Royal Society of Chemistry. (f) Optical image of A (3TE:EDOT = 3:1), B (3TE:EDOT = 3:2), C (3TE:EDOT = 3:3), D (3TE:EDOT = 2:3), and E (3TE:EDOT = 1:3) samples.[88] Reproduced with permission from Goktas *et al.*, J. Mater. Chem. C **4**, 3403 (2016). Copyright 2016 Royal Society of Chemistry. (g) Photo images of the copolymer of poly(ANTH-co-EDOT) and poly(BPH-co-EDOT) and the typical homopolymer of PEDOT on glass slides.[89] Reproduced with permission from Lee and Gleason, Adv. Funct. Mater. **25**, 85 (2015). Copyright 2015 Wiley-VCH. (h) Optical transmission spectra from ∼55 nm-thick samples investigated in the visible regime from 300 to 800 nm.[89] Reproduced with permission from Lee and Gleason, Adv. Funct. Mater. **25**, 85 (2015). Copyright 2015 Wiley-VCH.

from light yellow to dark blue, and the absorption (transparency) was increased (decreased), as demonstrated in Fig. 5(f).

Excellent transparency is vital when the copolymer is used in optical devices, such as photovoltaic cells, electrochromic windows, and light sensors. Of note, the transparency and other optical properties of copolymers can be easily engineered by facile copolymerization as well as controlling process parameters during the oCVD synthetic process. Lee and Gleason demonstrated oCVD engineering of the bandgap and optical properties of PEDOT by copolymerization with cross-linking monomers of biphenyl (BPH) and anthracene (ANTH), leading to copolymers, poly(BPH-co-EDOT) and poly(ANTH-co-EDOT), respectively [Fig. 5(g)].[89] Through the oCVD copolymerization, the bandgap of PEDOT was tuned in a range of 1.8–2.3 eV, and the visible optical transmittance was enhanced from 80% of the homopolymer PEDOT to 88% of poly(BPH-co-EDOT), and up to 93% of poly(ANTH-co-EDOT). Particularly, unlike the homopolymer PEDOT, the copolymers presented no degradation in the optical transmittance at the higher wavelength region [Fig. 5(h)], of which the enhanced visible optical performance is required in various organic optoelectronic applications such organic photovoltaics. The oCVD technique may be limited by relatively high initial facility cost, compared to other methods, and may not be desired to obtain bulk films with thicknesses greater than, for example, 10 μm.

VI. CONCLUSIONS AND OUTLOOK

In this perspective, we have summarized and described the synthetic methods of functional copolymers and applications in electronic, optical, and sensing devices with engineered physical properties. Reaction parameters during the synthesis process are discussed to identify the relationship with the desired physical properties of the copolymer. Reactants, applied voltages, currents, reaction time, and wavelengths of radiation govern the physical properties of the synthesized copolymer in those traditional polymerization processes. Hence, the desired physical properties of the synthesized copolymer can be achieved by changing one or several parameters of the synthesis process. In addition, practical and potential applications of synthesized copolymers with enhanced properties are provided in each synthesis method. Copolymers may find various applications due to the achieved multifunctional properties of bipolar electronic characteristics in switching and next-generation logic devices, organic solar cells, and photodetectors; the high conductivity with engineered surface properties for chemical sensors; and the enhanced optical properties with conductivity for transparent electrodes. These device applications typically require thin films of copolymers with conformal coverage and pinhole-free uniform surface, which is not often achieved by conventional solution-based processing. Emerging advanced synthesis methods, such as the oCVD technique have demonstrated a wide range of device applications with superior performance to those of conventional counterparts by addressing the requirements, which is expected to be a versatile approach for engineering electronic, optical, and optoelectronic properties through facile copolymerization. In addition to the electronic, optical, and sensing properties, the enhanced understanding of the process–structure–property relationship from this perspective may be of useful relevance to engineering other physical properties, such as mechanical and catalytic properties, which can also be engineered by the cross-linking and chain-end group modification through copolymerization.

ACKNOWLEDGMENTS

This work was partially supported by NSF, Award No. CBET-2207302. The authors greatly appreciate productive discussions and suggestions from Dr. Karen Gleason at M.I.T.

AUTHOR DECLARATIONS

Conflict of Interest

The authors have no conflicts to disclose.

Author Contributions

Yuxuan Zhang: Conceptualization (equal); Writing – original draft (equal); Writing – review & editing (equal). **Sunghwan Lee:** Conceptualization (lead); Funding acquisition (lead); Supervision (lead); Writing – review & editing (lead).

DATA AVAILABILITY

Data sharing is not applicable to this article as no new data were created or analyzed in this study.

REFERENCES

[1]T. Cedervall, I. Lynch, S. Lindman, T. Berggård, E. Thulin, H. Nilsson, K. A. Dawson, and S. Linse, Proc. Natl. Acad. Sci. U. S. A. **104**(7), 2050 (2007).
[2]P. Król, Prog. Mater. Sci. **52**(6), 915 (2007).
[3]C. Liang, K. Hong, G. A. Guiochon, J. W. Mays, and S. Dai, Angew. Chem., Int. Ed. **43**(43), 5785 (2004).
[4]P. Alexandridis, J. F. Holzwarth, and T. A. Hatton, Macromolecules **27**(9), 2414 (1994).
[5]J. A. Brydson, *Plastics Materials*, 7th ed. (Butterworth-Heinemann, Oxford, 1999), p. 694.
[6]A. Shrivastava, *Introduction to Plastics Engineering* (William Andrew Publishing, 2018), p. 17.
[7]D. Wu, F. Xu, B. Sun, R. Fu, H. He, and K. Matyjaszewski, Chem. Rev. **112**(7), 3959 (2012).
[8]A. M. Coclite, R. M. Howden, D. C. Borrelli, C. D. Petruczok, R. Yang, J. L. Yagüe, A. Ugur, N. Chen, S. Lee, W. J. Jo, A. Liu, X. Wang, and K. K. Gleason, Adv. Mater. **25**(38), 5392 (2013).
[9]S. Stankovich, D. A. Dikin, G. H. B. Dommett, K. M. Kohlhaas, E. J. Zimney, E. A. Stach, R. D. Piner, S. T. Nguyen, and R. S. Ruoff, Nature **442**(7100), 282 (2006).
[10]D.-W. Wang, F. Li, J. Zhao, W. Ren, Z.-G. Chen, J. Tan, Z.-S. Wu, I. Gentle, G. Q. Lu, and H.-M. Cheng, ACS Nano **3**(7), 1745 (2009).
[11]Y. Yagci, S. Jockusch, and N. J. Turro, Macromolecules **43**(15), 6245 (2010).
[12]W. E. Tenhaeff and K. K. Gleason, Adv. Funct. Mater. **18**(7), 979 (2008).
[13]A. Khlyustova, Y. Cheng, and R. Yang, J. Mater. Chem. B **8**(31), 6588 (2020).
[14]Q.-F. Lü, M.-R. Huang, and X.-G. Li, Chem. Eur. J. **13**(21), 6009 (2007).
[15]X.-G. Li, Q.-F. Lü, and M.-R. Huang, Small **4**(8), 1201 (2008).
[16]T. Yokozawa and Y. Ohta, Chem. Rev. **116**(4), 1950 (2016).
[17]A. Yokoyama and T. Yokozawa, Macromolecules **40**(12), 4093 (2007).
[18]A. Yokoyama, R. Miyakoshi, and T. Yokozawa, Macromolecules **37**(4), 1169 (2004).
[19]E. E. Sheina, J. Liu, M. C. Iovu, D. W. Laird, and R. D. McCullough, Macromolecules **37**(10), 3526 (2004).
[20]A. Sunder, J. Heinemann, and H. Frey, Chem. Eur. J. **6**(14), 2499 (2000).
[21]D. Colombani, Prog. Polym. Sci. **22**(8), 1649 (1997).
[22]K. Liu, Z. Nie, N. Zhao, W. Li, M. Rubinstein, and E. Kumacheva, Science **329**(5988), 197 (2010).
[23]J. Kang, D. Miyajima, T. Mori, Y. Inoue, Y. Itoh, and T. Aida, Science **347**(6222), 646 (2015).
[24]M. P. Stevens, *Polymer Chemistry* (Oxford University Press, New York, 1990).
[25]A. Rudin, *Elements of Polymer Science and Engineering*, 2nd ed. (Academic Press, San Diego, 1999), p. 155.
[26]A. Rudin and P. Choi, *The Elements of Polymer Science & Engineering*, 3rd ed. (Academic Press, Boston, MA, 2013), p. 305.
[27]J. K. Hitt, T. G. Sugar, M. Holgate, and R. Bellman, J. Med. Devices **4**(1), 011003 (2010).
[28]T. Kelen and F. TÜds, J. Macromol. Sci.: Part A **9**(1), 1 (1975).
[29]S. D. Ittel, L. K. Johnson, and M. Brookhart, Chem. Rev. **100**(4), 1169 (2000).
[30]G. H. Fredrickson and F. S. Bates, Annu. Rev. Mater. Sci. **26**(1), 501 (1996).
[31]A. D. Jenkins, P. Kratochvíl, R. F. T. Stepto, and U. W. Suter, Pure Appl. Chem. **68**(12), 2287 (1996).
[32]H. Takahashi, G. A. Caputo, S. Vemparala, and K. Kuroda, Bioconjugate Chem. **28**(5), 1340 (2017).
[33]G. Riess, Prog. Polym. Sci. **28**(7), 1107 (2003).
[34]J. Huang and S. Richard Turner, Polymer **116**, 572 (2017).
[35]M. Trollsås, M. A. Kelly, H. Claesson, R. Siemens, and J. L. Hedrick, Macromolecules **32**(15), 4917 (1999).
[36]Y. Tsujii, K. Ohno, S. Yamamoto, A. Goto, and T. Fukuda, in *Surface-Initiated Polymerization I*, edited by R. Jordan (Springer Berlin Heidelberg, Berlin, Heidelberg, 2006), pp. 1.
[37]F. R. Mayo and F. M. Lewis, J. Am. Chem. Soc. **66**(9), 1594 (1944).
[38]D. Zhao, Q. Huo, J. Feng, B. F. Chmelka, and G. D. Stucky, J. Am. Chem. Soc. **120**(24), 6024 (1998).
[39]H. Maeda, J. Wu, T. Sawa, Y. Matsumura, and K. Hori, J. Controlled Release **65**(1), 271 (2000).
[40]J. Cho, J. Hong, K. Char, and F. Caruso, J. Am. Chem. Soc. **128**(30), 9935 (2006).

[41]A. R. Kim and D. J. Yoo, Polymers **11**, 1264 (2019).
[42]M. H. Gharahcheshmeh and K. K. Gleason, Adv. Mater. Interfaces **6**(1), 1801564 (2019).
[43]T. A. Saleh, *Polymer Hybrid Materials and Nanocomposites* (William Andrew Publishing, 2021), p. 177.
[44]A. de Leon and R. C. Advincula, in *Intelligent Coatings for Corrosion Control*, edited by A. Tiwari, J. Rawlins, and L. H. Hihara (Butterworth-Heinemann, Boston, MA, 2015), p. 409.
[45]O. N. Oliveira, M. Raposo, and A. Dhanabalan, in *Handbook of Surfaces and Interfaces of Materials*, edited by H. S. Nalwa (Academic Press, Burlington, 2001), p. 1.
[46]Y. Q. Gill, U. Abid, U. Mehmood, A. Ishfaq, M. B. Naqviin *et al.*, *Polymer Nanocomposites Containing Graphene*, edited by M. Rahaman, L. Nayak, and I. A. Hussein (Woodhead Publishing, 2022), p. 425.
[47]C. Schotten, T. P. Nicholls, R. A. Bourne, N. Kapur, B. N. Nguyen, and C. E. Willans, Green Chem. **22**(11), 3358 (2020).
[48]J. H. Kaufman, K. Keiji Kanazawa, and G. B. Street, Phys. Rev. Lett. **53**(26), 2461 (1984).
[49]J. Anand, S. Palaniappan, and D. N. Sathyanarayana, Prog. Polym. Sci. **23**(6), 993 (1998).
[50]J. Heinze, A. Rasche, M. Pagels, and B. Geschke, J. Phys. Chem. B **111**(5), 989 (2007).
[51]T. F. Otero and E. De Larreta, Synth. Met. **26**(1), 79 (1988).
[52]J. V. Sanchez, R. Diaz, P. Herrasti, and P. Ocon, Polym. J. **33**(7), 514 (2001).
[53]M. Velazquez Rosenthal, T. A. Skotheim, A. Melo, M. I. Florit, and M. Salmon, J. Electroanal. Chem. Interfacial Electrochem. **185**(2), 297 (1985).
[54]S. Naitoh, K. Sanui, and N. Ogata, J. Chem. Soc, Chem. Commun. **15**(17), 1348 (1986).
[55]K. Shi, H. Zou, B. Sun, P. Jiang, J. He, and X. Huang, Adv. Funct. Mater. **30**(4), 1904536 (2020).
[56]K. Liu, Z. Hu, R. Xue, J. Zhang, and J. Zhu, J. Power Sources **179**(2), 858 (2008).
[57]M.-Y. Chou, M-k Leung, Y. O. Su, C. L. Chiang, C.-C. Lin, J.-H. Liu, C.-K. Kuo, and C.-Y. Mou, Chem. Mater. **16**(4), 654 (2004).
[58]Y. Dai, W. Li, X. Qu, J. Liu, S. Yan, M. Ouyang, X. Lv, and C. Zhang, Electrochim. Acta **229**, 271 (2017).
[59]S. Wustoni, T. C. Hidalgo, A. Hama, D. Ohayon, A. Savva, N. Wei, N. Wehbe, and S. Inal, Adv. Mater. Technol. **5**(3), 1900943 (2020).
[60]Z. C. Hern, S. M. Quan, R. Dai, A. Lai, Y. Wang, C. Liu, and P. L. Diaconescu, J. Am. Chem. Soc. **143**(47), 19802 (2021).
[61]Y. Yuan and A. Lei, Nat. Commun. **11**(1), 802 (2020).
[62]D. Gust and T. A. Moore, Science **244**(4900), 35 (1989).
[63]C. Decker, Prog. Polym. Sci. **21**(4), 593 (1996).
[64]J. Shao, Y. Huang, and Q. Fan, Polym. Chem. **5**(14), 4195 (2014).
[65]A. Reiche, R. Sandner, A. Weinkauf, B. Sandner, G. Fleischer, and F. Rittig, Polymer **41**(10), 3821 (2000).
[66]C. C. McClain, C. G. Brown, J. Flowers, V. Q. Nguyen, and D. A. Boyd, Ind. Eng. Chem. Res. **57**(27), 8902 (2018).
[67]M. Knaapila, H. Høyer, J. Kjelstrup-Hansen, and G. Helgesen, ACS Appl. Mater. Interfaces **6**(5), 3469 (2014).
[68]A. Bagheri and J. Jin, ACS Appl. Polym. Mater. **1**(4), 593 (2019).
[69]K. K. Gleason, *CVD Polymers: Fabrication of Organic Surfaces and Devices* (John Wiley & Sons, 2015).
[70]S. Lee, D. C. Borrelli, W. J. Jo, A. S. Reed, and K. K. Gleason, Adv. Mater. Interfaces **5**(9), 1870041 (2018).
[71]J. P. Lock, S. G. Im, and K. K. Gleason, Macromolecules **39**(16), 5326 (2006).
[72]S. G. Im and K. K. Gleason, Macromolecules **40**(18), 6552 (2007).
[73]M. H. Gharahcheshmeh, M. M. Tavakoli, E. F. Gleason, M. T. Robinson, J. Kong, and K. K. Gleason, Sci. Adv. **5**(11), eaay0414 (2019).
[74]B. Reeja-Jayan, P. Kovacik, R. Yang, H. Sojoudi, A. Ugur, D. H. Kim, C. D. Petruczok, X. Wang, A. Liu, and K. K. Gleason, Adv. Mater. Interfaces **1**(4), 1400117 (2014).
[75]X. Wang, X. Zhang, L. Sun, D. Lee, S. Lee, M. Wang, J. Zhao, Y. Shao-Horn, M. Dincă, T. Palacios, and K. K. Gleason, Sci. Adv. **4**(9), eaat5780 (2018).
[76]S. H. Baxamusa, S. G. Im, and K. K. Gleason, Phys. Chem. Chem. Phys. **11**(26), 5227 (2009).
[77]A. Asatekin, M. C. Barr, S. H. Baxamusa, K. K. S. Lau, W. Tenhaeff, J. Xu, and K. K. Gleason, Mater. Today **13**(5), 26 (2010).
[78]Y. Zhang, C. S. Kim, H. W. Song, S.-J. Chang, H. Kim, J. Park, S. Hu, K. Zhao, and S. Lee, Energy Storage Mater. **48**, 1 (2022).
[79]M. Clevenger, H. Kim, H. W. Song, K. No, and S. Lee, Sci. Adv. **7**(42), eabj8958 (2021).
[80]M. E. Alf, A. Asatekin, M. C. Barr, S. H. Baxamusa, H. Chelawat, G. Ozaydin-Ince, C. D. Petruczok, R. Sreenivasan, W. E. Tenhaeff, N. J. Trujillo, S. Vaddiraju, J. Xu, and K. K. Gleason, Adv. Mater. **22**(18), 1993 (2009).
[81]S. G. Im, D. Kusters, W. Choi, S. H. Baxamusa, M. C. M. van de Sanden, and K. K. Gleason, ACS Nano **2**(9), 1959 (2008).
[82]M. M. Tavakoli, M. H. Gharahcheshmeh, N. Moody, M. G. Bawendi, K. K. Gleason, and J. Kong, Adv. Mater. Interfaces **7**(16), 2000498 (2020).
[83]S. Vaddiraju, K. Seneca, and K. K. Gleason, Adv. Funct. Mater. **18**(13), 1929 (2008).
[84]S. Vaddiraju and K. K. Gleason, Nanotechnology **21**(12), 125503 (2010).
[85]D. Bhattacharyya and K. K. Gleason, Chem. Mater. **23**(10), 2600 (2011).
[86]D. Bhattacharyya, K. Senecal, P. Marek, A. Senecal, and K. K. Gleason, Adv. Funct. Mater. **21**(22), 4328 (2011).
[87]A. Hebert, M. Bishop, D. Bhattacharyya, K. Gleason, and S. Torosian, Appl. Nanosci. **5**(6), 763 (2015).
[88]H. Goktas, X. Wang, N. D. Boscher, S. Torosian, and K. K. Gleason, J. Mater. Chem. C **4**(16), 3403 (2016).
[89]S. Lee and K. K. Gleason, Adv. Funct. Mater. **25**(1), 85 (2015).